Received October 2003
Reviewed November 2004
Accepted July 2005

Jet entrainment minimization in an air curtain of open refrigerated display case

Homayun K. Navaz
Mechanical Engineering Department, Kettering University, Flint, Michigan, USA
Mazyar Amin
Aeronautics and Astronautics Engineering Department, University of Washington, Seattle, Washington, USA
Srinivasan C. Rasipuram
Mechanical Engineering Department, Kettering University, Flint, Michigan, USA, and
Ramin Faramarzi
Southern California Edison Company, Irwindale, California, USA

Abstract

Purpose – To address the effects of velocity profile at the discharge air grille (DAG) on the amount of entrained air into an open refrigerated display case (ORDC).

Design/methodology/approach – The performance of an ORDC was studied by CFD, DPIV and LDV. The actual measured velocity profile at the DAG and total flow rate of the display case at its nominal operating conditions are used as guidelines throughout the CFD modeling.

Findings – It was found that a skewed parabolic profile with the peak shifted towards the inner section of the case generates the minimum entrainment and demonstrates that with simple changes to the geometry of the DAG, a significant reduction in the entrainment rate could be achieved.

Research limitations/implications – This study finds the optimum infiltration rate of a manufactured ORDC. A fundamental study is currently being done to address all the effective parameters that can affect the infiltration rate of any ORDCs.

Originality/value – This paper presents this fact that the velocity profile at the DAG has a significant impact on the infiltration rate and electricity consumption of ORDCs. In turn, the velocity profile is dependent on the geometry and shape of the air passage before DAG. Thus, the analysis of the effect of the geometry on the velocity should seriously be taken into consideration by the case manufacturers.

Keywords Jets, Air, Velocity measurement

Paper type Research paper

Introduction

Open refrigerated display cases (ORDCs) are used in supermarkets to maintain the food products at prescribed temperatures. Cold air is provided through an inlet jet

This work was sponsored in part by the US Department of Energy, Office of Building Technology, State and Community Programs under contract DE-AC05-00OR22725 with UT-Battelle, LLC.

International Journal of Numerical Methods for Heat & Fluid Flow
Vol. 16 No. 4, 2006
pp. 417-430

0961-5539
DOI 10.1108/09615530610653064

called the discharge air grille (DAG) located at the top front of the unit and through a group of slots located on the back panel of the case. The cold air jet at the top forms an invisible barrier between the outside warm air and the cold air inside the display case and enters the return air grille (RAG) located on the front and lower part of the display case. This invisible barrier is called the air curtain and depending on its characteristics (shape, turbulence intensity, velocity, etc.) at the point of origination (i.e. the DAG) controls the amount of outside warm air that is pulled into the mixing zone. The continuous flow of warm air into the air curtain and its subsequent mixing with cold air is called entrainment. A portion of the entrained air spills over after some mixing with the cold air, and the rest is infiltrated into the RAG after it has increased the cold air temperature and thereafter imposes a cooling load on the refrigeration cycle. Obviously, the amount of infiltrated warm air should be kept to a minimum to conserve energy for running the cooling cycle to maintain a prescribed cold air temperature that is being driven to the DAG and the back panel.

Earlier studies of the air curtain (Howell and Adams, 1991) describe the importance of the inlet velocity and eddy viscosity that is created in the presence of turbulence. Although the study is informative it uses simplistic models to express the eddy viscosity and fluid mechanics of the display case. According to Howell and Adams (1991), 75 percent of the refrigeration load is induced by the air curtain entrainment.

Combining analytical and experimental methods to understand the behavior of air curtains started during the 1960s. The works of Hetsroni *et al.* (1963) are based on the laminar formulation of the boundary layer equations with body forces to study buoyancy effect. The non-dimensional analysis was then used to group all parameters, and finally, through the data gathering, obtain proper coefficients for correlation-based formulation. Although such techniques are useful for a "global" understanding of jets or air curtains, they are incapable of providing detailed information.

Stribling *et al.* (1999) have made an attempt to combine more modern analysis tools (i.e. computational fluid dynamics (CFD) and experimental results) to study the velocity and turbulence in a display case. Their research indicated a good qualitative agreement but demonstrates some quantitative discrepancies between the experimental and computational results.

In a recent study (Navaz *et al.*, 2002), digital particle image velocimetry (DPIV) and CFD tools were used to study the dependency of the entrainment rate of the air curtain on the DAG velocity and temperature, and showed that the mixing and entrainment are mostly momentum driven and buoyancy effects are negligible for the operating conditions of typical display cases. It has also been shown that this modern hybrid approach not only generates correlation-based equations for entrainment rate, but also produces detailed information about the velocity field used to analyze turbulence effects. Furthermore, calibration of CFD model with experimental results to define correct boundary conditions for parametric studies is a prelude for correct and accurate parametric studies for the purpose of optimizing the air curtain performance.

The effect of the Richardson and Reynolds numbers on the shape of the streamlines representing the entrained air at the DAG was studied too (Field *et al.*, 2002). This study attempted to eliminate case-specific issues (i.e. the DAG width and velocity unique to each manufacturer). However, it did not address and quantify the DAG turbulence issues. It also concluded that the buoyancy effects will become significant for a Reynolds number less than or equal to 100.

Navaz *et al.* (2004) have studied the effects of the turbulence intensity and Reynolds number based on the DAG average velocity and width on the entrainment rate of a specific display case. Their results point towards an optimum Reynolds number to minimize the entrainment rate. They also showed that turbulence intensity increases significantly at the DAG due to the existence of multiple maxima of the velocity profile at the DAG. This increase is due to the shear that arises from the two-jet configuration and contributes to an increased entrainment rate. They showed that the amount of the infiltrated air into the RAG is a function of the cold and warm temperatures along with the average temperature of the over spilled air, and the average temperature at the RAG. As a rule of thumb the infiltrated air is about 33 percent of the total entrained air.

The previous study (Navaz *et al.*, 2004) pointed out that the Reynolds number and the turbulence intensity that can be a result of the shape of the velocity profile at the DAG are controlling the entrainment rate. The present study takes a systematic approach towards understanding and quantifying the entrainment rate as a function of the velocity profile, and attempts to identify the DAG geometry that can produce the best velocity profile and reduced entrainment rate thereafter.

Model

The testing was performed in $6\,\mathrm{m} \times 2.55\,\mathrm{m} \times 2.25\,\mathrm{m}$ controlled temperature room. In the previous studies (Navaz *et al.*, 2002, 2004), the velocity profile at the DAG was experimentally determined at several longitudinal locations (along the length of the display case) and it was determined that the velocity profile remains essentially unchanged, therefore, justifying a two-dimensional computational analysis. A general schematic of the cross section of our particular display case in the actual testing chamber is shown in Figure 1. The cold air is provided to the display case through the DAG and perforated back panel with numerous slots. The mixing of the cold air curtain and outside warm air starts shortly after the departure of the flow from the DAG. A mixture of the cold and warm air reaches the RAG where it is run over the coils for re-cooling. The CFD analysis was performed for two separate domains:

(1) Inside the display case, i.e. flow entering the RAG over the coils, through the back panel and plenum, and leaving the computational domain at the DAG, and perforated back panel slots.

(2) Outside the display case and the room using the flow through the back panel and DAG as inlets and the flow through the RAG as outlet. The left boundary of the computational domain is determined as a constant temperature volume at prescribed room temperature of 23.9°C (75°F).

The purpose of part (1) is to ensure that the "inside" geometry of the display case will produce the velocity profile at the DAG that is being measured by laser doppler velocimetry (LDV) and DPIV a short distance 5 cm (2 in) outside the DAG. That is to say that the velocity profile at the DAG extracted from the CFD solution for part (1) should resemble to what the measurements show. Although they are not going to be identical because the experimental values obtained by DPIV or LDV are at 5 cm (2 in) below the DAG, their similarity will increase our confidence in the CFD analysis performed for the inner part of the display case. Furthermore, the accurate prediction of the velocity profile at the DAG will ensure our modeling of grouping the flow through the perforated back panel. On the other hand, the validation of the velocity profile at

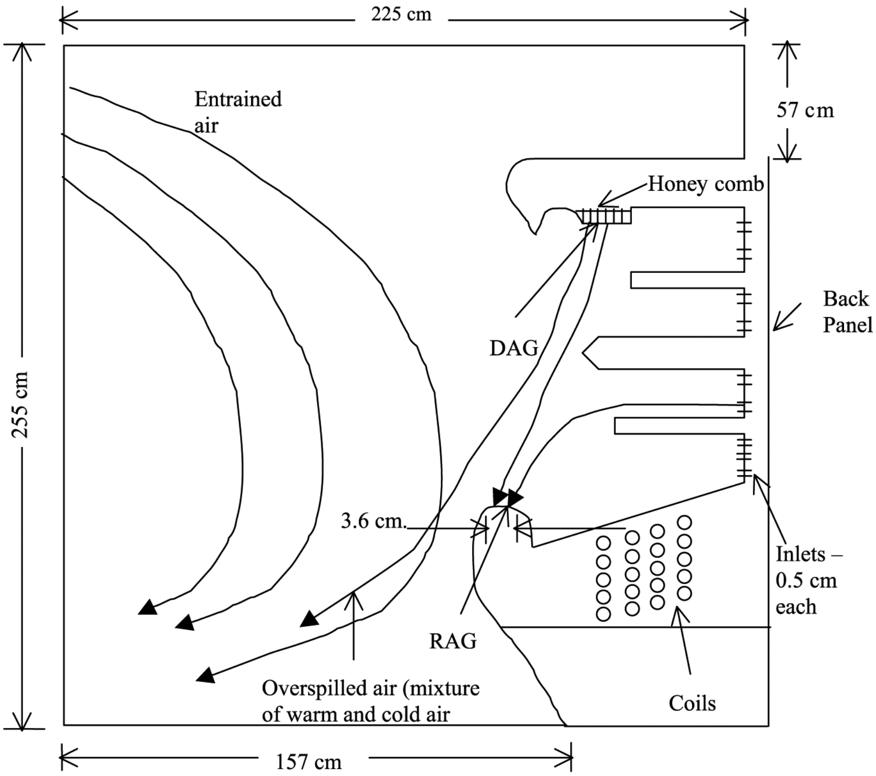

Figure 1.
A general schematic of the display case with major dimensions

the DAG for the given geometry will enhance our confidence in the resulted DAG velocity after the alteration of its geometry to obtain the "best" velocity profile at the DAG for minimizing the entrainment.

Obviously the purpose of part (b) is to calculate the entrainment rate based on the velocity profile at the DAG.

For part (1) CFD analysis, RAG is an inlet boundary, and flow through the back panel and DAG represents the outflow conditions. The dimensions of individual slots on the back panel were measured and the total perforated area on the back panel was calculated. Then, the total area was divided into two or three outlets depending on where the shelves were mounted. By knowing the length of the display case 2.44 m (8 ft), the two-dimensional representation of all outlets (lumped) on the back panel was calculated and used in the computational model. To obtain the total volumetric flow rate through the display case, a part of the metal casing of the RAG was replaced by Plexiglas and the LDV technique was used to map the velocity profile inside the RAG channel. By knowing the total area of the RAG and calculating the average velocity, a total flow rate of 26.4 m^3/min (930 cfm) was obtained of which 26.9 percent is discharged from the top (7.1 m^3/min or 250 cfm) at the DAG specified by mapping the velocity profile by the DPIV method, and the rest from the back panel. This is the actual flow rate in what is being referred to as the "base" "actual" or "original" case hereinafter. It is also assumed that the velocity through the back panel is uniform across each slot in the model that is a representation of a group of slots in the real case.

It was mentioned earlier that the main focus of this work is the effect of the velocity profile at the DAG or the jet exit plane on the entrainment of the outside air. However, since the same mean velocity profile could possess different turbulence intensity due to the fluctuations present in the flow, another variable that is considered in this study is the turbulence intensity at inlets. The CFD model provides a solution for Navier-Stokes equations with turbulence being expressed by the low Reynolds number k-ε two-equation model. The law-of-the wall is applied for near wall region.

Results

Before engaging in parts (1) and (2) of this research, the issue that can be put forward is the contribution of turbulence intensity of the back panel flow to the entrainment rate. Although our previous studies (Navaz *et al.*, 2002, 2004) have indicated that a major portion of the back panel flow is returned to the cooling coils without considerable amount of mixing with the outside warm air, quantification of this contribution will complement our research effort and provides better understanding of air curtains. Our previous research also indicated that the optimum operating Reynolds number at the DAG is about 3,400. This Reynolds number delays the development of turbulence along the air curtain and yet has enough momentum to prevent the premature spreading of the air curtain before it reaches the RAG. The optimum Reynolds number of 3,400 refers to a total display case volumetric flow rate of 21.24 m^3/min (750 cfm) with the volumetric flow rate of 5.95 m^3/min (210 cfm) at the DAG. Since this is the Reynolds number that we are aiming for, some of our parametric studies are performed using these values instead of the “actual” operating conditions.

The back panel flow acts mostly like a stabilizer (for the food product temperature), after the air curtain is broken by customers reaching to the shelves. It also fortifies the air curtain with the entrained air by sandwiching effects. However, we need to demonstrate that the role of the back panel flow conditions is significantly smaller than that of the DAG. A series of computer runs for the outside flow (part 2) were performed for several DAG Reynolds numbers (based on the DAG width) ranging from 3,000 to 6,000. The four cases are:

(1) Fully laminar flow – throughout the computational domain and all inlets, i.e. DAG and back panel flows enter the domain possessing no turbulence intensity.

(2) Turbulence is allowed to develop throughout the computational domain, but the flow is entering the domain at DAG and back panel with no turbulence intensity.

(3) Turbulence is allowed to develop throughout the computational domain but the flow is entering the domain with 20 percent turbulence intensity from the back panel and no turbulence (laminar) through the DAG.

(4) Turbulence is allowed to develop throughout the computational domain and the flow is entering the domain with 20 percent turbulence intensity at all inlets (i.e. back panel and DAG).

Figure 2 shows a plot of computed normalized entrainment rate (entrainment rate/total flow rate) as a function of the Reynolds number at the DAG for all four cases just

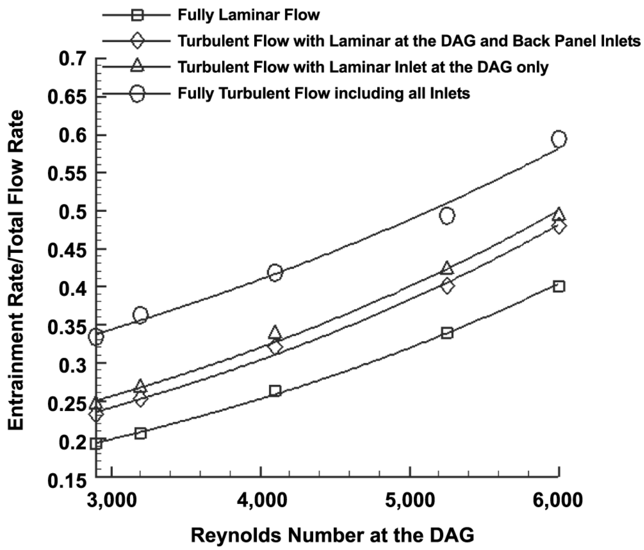

Figure 2.
Entrainment rate as a function of Reynolds number for different inflow conditions at the inlets

mentioned. It is obvious that a fully laminar flow (not practical) entrains the minimum amount of warm air. When the turbulence is allowed to be developed in the domain, the entrainment rate becomes a function of the turbulence intensity at inlets. It is seen that by introducing turbulence at the back panel inflow, the entrainment rate does not differ much from the flow where laminar inlet conditions is assumed. Finally, introducing turbulence at the DAG will significantly increase the entrainment rate. We can conclude that achieving laminar flow through the back panel will not contribute to minimizing the entrainment rate. However, design of a laminar flow at the DAG will noticeably decrease the entrainment rate. Therefore, the contribution of the back panel flow to entrainment rate is second order next to that of the DAG.

Now we are going to focus on the effects of the DAG exit flow conditions on the entrainment rate. In the previous work (Navaz *et al.*, 2004) we pointed out that the two maxima that were observed in the mean vertical velocity profile at the DAG could be a source of turbulent kinetic energy production and thus increased entrainment. We also mentioned that the velocity at the DAG should have only one peak; eliminating the possibility of turbulence production due to shear effects that arise from multiple-peak velocity profiles thus resembling to a fully laminar flow. It is obvious that there are practical constraints that prevent us from creating a fully laminar flow at the DAG. Therefore, it may be asked “What is the best velocity profile that can be practically generated at the DAG causing a significant reduction in the entrainment rate?” To answer this question we have imposed several velocity profiles at the DAG including an actual measured velocity distribution. Each has the nominal Reynolds number of 4,300. This Reynolds number refers to the actual total display case flow rate of 26.4 m^3/min (930 cfm). The computational domain consists of the room (part 2) and the back panel and DAG are considered to be inlets. We have also imposed several turbulence intensity values at the DAG for each assumed or actual profile.

Figure 3 shows a schematic of all velocity profiles that have been considered. All scenarios in Figure 3 are simulated by CFD for different turbulence intensities

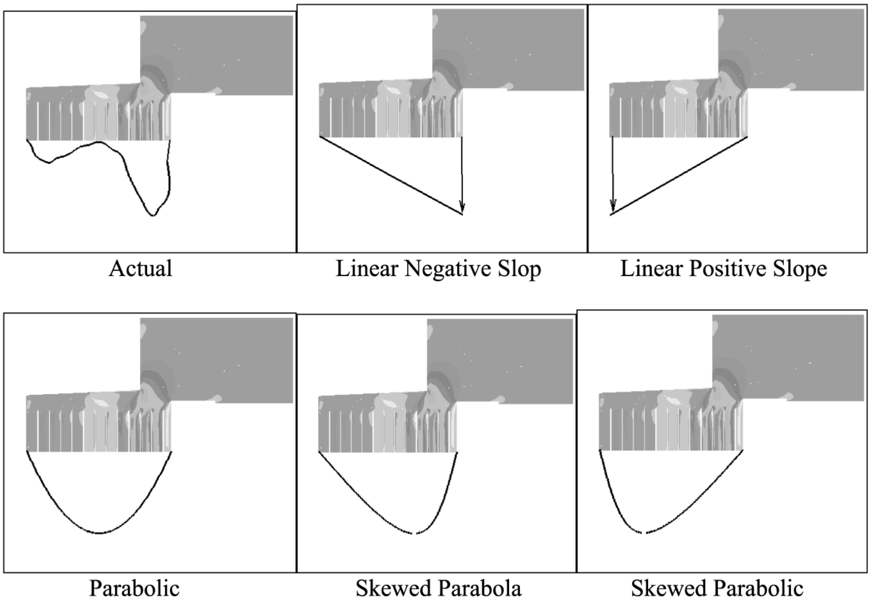

Figure 3.
Assumed DAG velocity profiles used in numerical simulation

imposed at the DAG, and the results for the normalized entrainment rate are shown in Figure 4. It can be observed that the linear profile with a negative slope generates the best results, i.e. has the least amount of entrainment. However, generating a Couette flow type (negative or positive slope) is not practical. By the same token, considering the geometry of the DAG region that is displayed in Figure 3

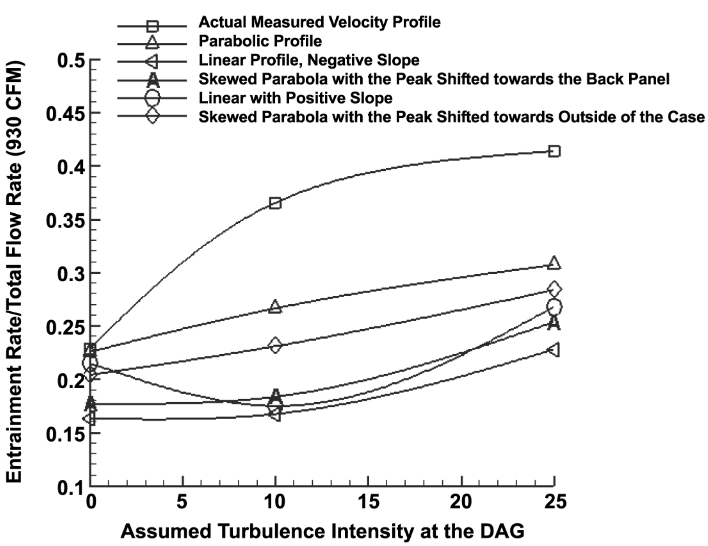

Figure 4.
Entrainment rate as a function of imposed turbulence intensity and different velocity profiles at the DAG ($Re_{DAG} = 4,300$)

(flow moving from right to left) generating a perfect parabolic profile also seems to be unrealistic. Furthermore, by examining the actual velocity profile, we postulate that the most practical velocity profile that can be achieved at the DAG is a skewed parabola with the peak shifted towards the back panel (or right in Figure 3) of the display case. By examining the results of Figure 4, it is evident that the skewed parabolic profile at the DAG, with the peak shifted towards the inside of the display case (back panel), generates the minimum entrainment rate next to the linear profile with negative slope. Therefore, based on these results, our goal is to produce a skewed parabolic profile at the DAG with its peak shifted towards the inside of the display case. The skewness can be mainly attributed to the asymmetrical geometry of the display case.

It is evident that the geometry of the flow before the DAG exit plane (i.e. the ducts and channels in the back of a display case) is coupled with the shape and characteristics of the velocity profile at the DAG. Therefore, the idea of varying the ductwork geometry before the DAG exit is how the desired velocity distribution can be achieved. On the other hand, before varying the geometry we should develop some confidence in the shape and characteristics of the velocity profile that we are going to obtain as a result of the DAG geometrical variations. This necessity prompted us to model the flow through the plenum and all the ductworks in the back of the display case, i.e. part (a) of our studies. The end result of this modeling is that the velocity profile at the DAG exit plane should be "compatible" with previously visualized and measured data. It should be noted that the velocity at the exit plane of the DAG is not going to be exactly what is measured about 5 cm (2 in) below the DAG (spreading of the jet already has occurred), however, if the two velocity profiles are close, we can have confidence in our CFD analysis for part (1), i.e. inside the ductwork.

The CFD modeling for the domain of part (1) was performed for the actual Reynolds number of 4,300 and postulated optimal Reynolds number of 3,400. If the same velocity profile (not magnitude just the profile) at the exit plane of the DAG is obtained for both Reynolds numbers, we can postulate that for all practical and operating Reynolds numbers, the geometry of the ductwork in the DAG region is mainly responsible for the shape of the velocity profile at the exit plane of the DAG. Figure 5 shows the result of the flow field modeling through the display case plenum and all the ductwork. The coils are modeled as 1.25 cm (0.5 in) circular obstructions in a staggered arrangement that was transferred from the actual CAD file. The velocity vectors at exits and contours of vertical velocity components are also shown in Figure 5. The flow enters the RAG through an area of about 0.0929 m^2 (1 ft^2) that reflects an average velocity of 283.49 m/min (930 ft/min) for the actual case ($Re = 4,300$) and 228.60 m/min (750 ft/min) for the scenario with DAG Reynolds number of 3,400. In both cases we have modeled the honeycomb as a set of parallel passages. By examining the vectors at the DAG we can identify a profile with two peaks similar to the observed velocity in our experimental work. The DAG and back panel slots are modeled as outlets and the velocity profiles at these locations is a result of our calculations.

Figure 6 shows the velocity profile at the DAG as extracted from Figure 5 for both of the above cases, and compares them to the measured data by LDV and DPIV techniques. They all have the same trend and can be interpreted as an excellent comparison. It should, however, be noted that the measured velocity profile is taken at about 5 cm (2 in) below the exit plane of the DAG after some spreading of the flow has

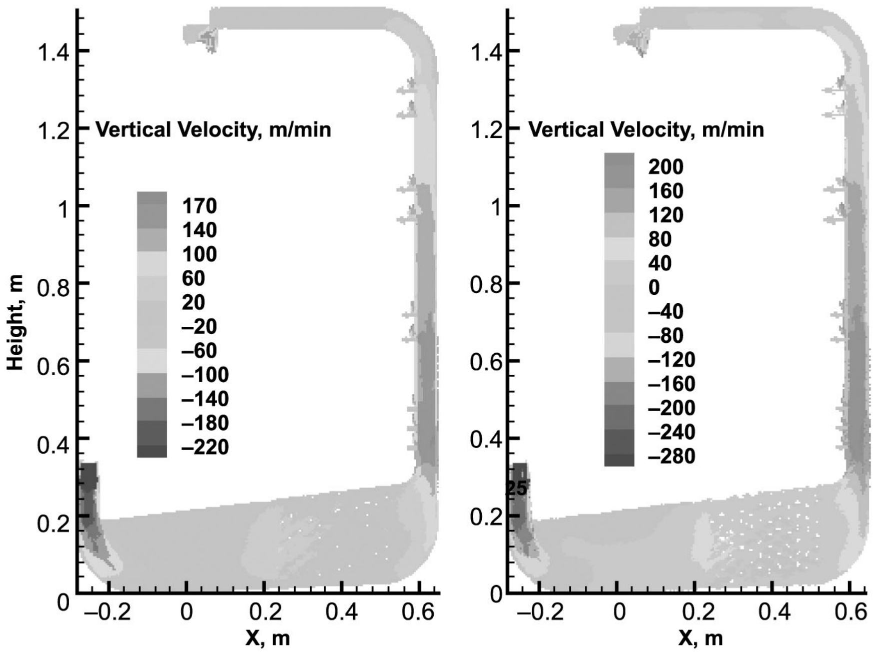

Figure 5.
Vertical velocity contours throughout the plenum and at the DAG for two different total case flow rates, nominal (Re = 4, 300) and proposed (Re = 3, 400). Total volumetric flow rate = 750 cfm for the figure on the left and 930 cfm for the figure on the right

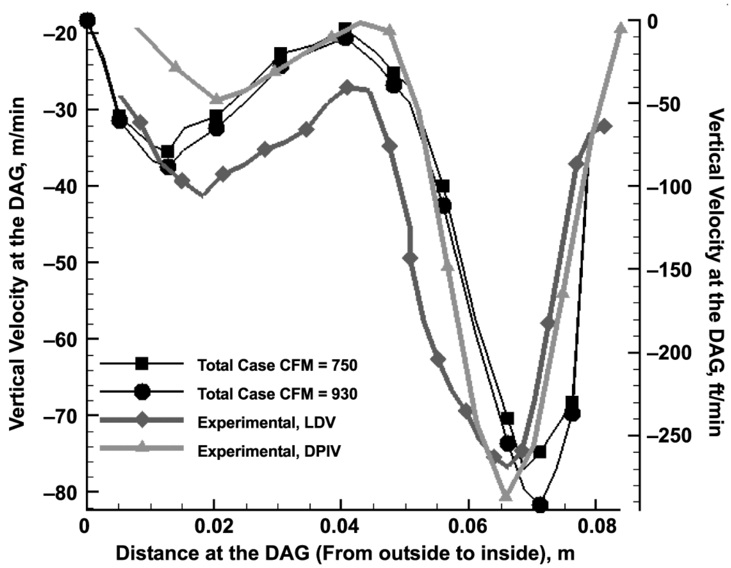

Figure 6.
The vertical velocity profile at the DAG inside the duct as predicted by numerical simulation and the observed profile outside the case by LDV and DPIV

already occurred. In spite of this fact, the results are satisfactory and the flow modeling throughout the back channels of the display case is acceptable and the analysis can be carried on further.

To eliminate the two-peak velocity profile configuration at the DAG that the original, or base-design generates, the vertical surface in the original design was replaced by a 20° slanted surface, postulating that the sudden change in the direction of the flow that can contribute to the creation of turbulence will be eliminated. This slope caused a shift of the main peak in velocity profile towards the outside of the display case, maintaining the two-peak configuration. Therefore, it was concluded that the best velocity profile that resembles a skewed parabola with the peak shifted towards the inside of the display case can be achieved with a slanted surface with an angle between 20° and 90° (original design). This angle was changed from 20° to 80° and after a series of computer simulations the optimum angle of 57° with a wider throat was obtained. Actual geometry, the 20° slanted surface, and the proposed design for minimum entrainment rate are shown in Figure 7. The reduction in turbulence kinetic energy that can be observed from Figure 7 confirms the fact that the best results can be obtained for the 57° slanted surface at the DAG. It is evident that we have attempted to obtain the optimum conditions with minimum and feasible changes that can be made to the present design.

In Figure 8, the velocity profile at the DAG exit for each case is shown and it is seen that the original case has two distinct peaks causing a shear between two layers of fluid that can trigger mixing. The 20° slanted surface profile seems to have a pronounced peak towards outside of the case with another small peak to the right. It appears that this case may be less effective than the original design. However, as the angle is changed to 57° and the flow passage area at the throat widened, significant improvement with respect to the shape of the velocity profile was observed.

Figure 8 shows a skewed parabolic profile with the peak shifted towards the inside of the display case for the proposed design. When the three velocity profiles were imposed as a boundary condition on a display case with a total volumetric flow rate of 750 cfm (Reynolds number based on DAG width = 3,400), it was observed that the 57° scenario yields the minimum entrainment for every turbulence intensity imposed at the DAG. Figure 9 shows the entrainment rate for all three cases at several turbulence intensity level imposed at the DAG. It is also seen that the entrainment worsens for the 20° slanted surface design due to the shape of the velocity profile at the DAG.

Furthermore, when the field turbulent kinetic energy contours are examined in Figure 10, it becomes clear that for the 57° scenario less turbulent kinetic energy develops within the outside field, therefore, reducing the amount of entrainment. So, we may conclude that the shape of the velocity profile at the DAG is of a great importance and can only be altered by changing the DAG duct geometry.

Conclusions

The complex flow configuration in the plenum of an ORDC is modeled, producing a velocity profile at the DAG similar to those visualized by DPIV and LDV methods. This validation test provided a calibrated CFD model for studying the effects of the

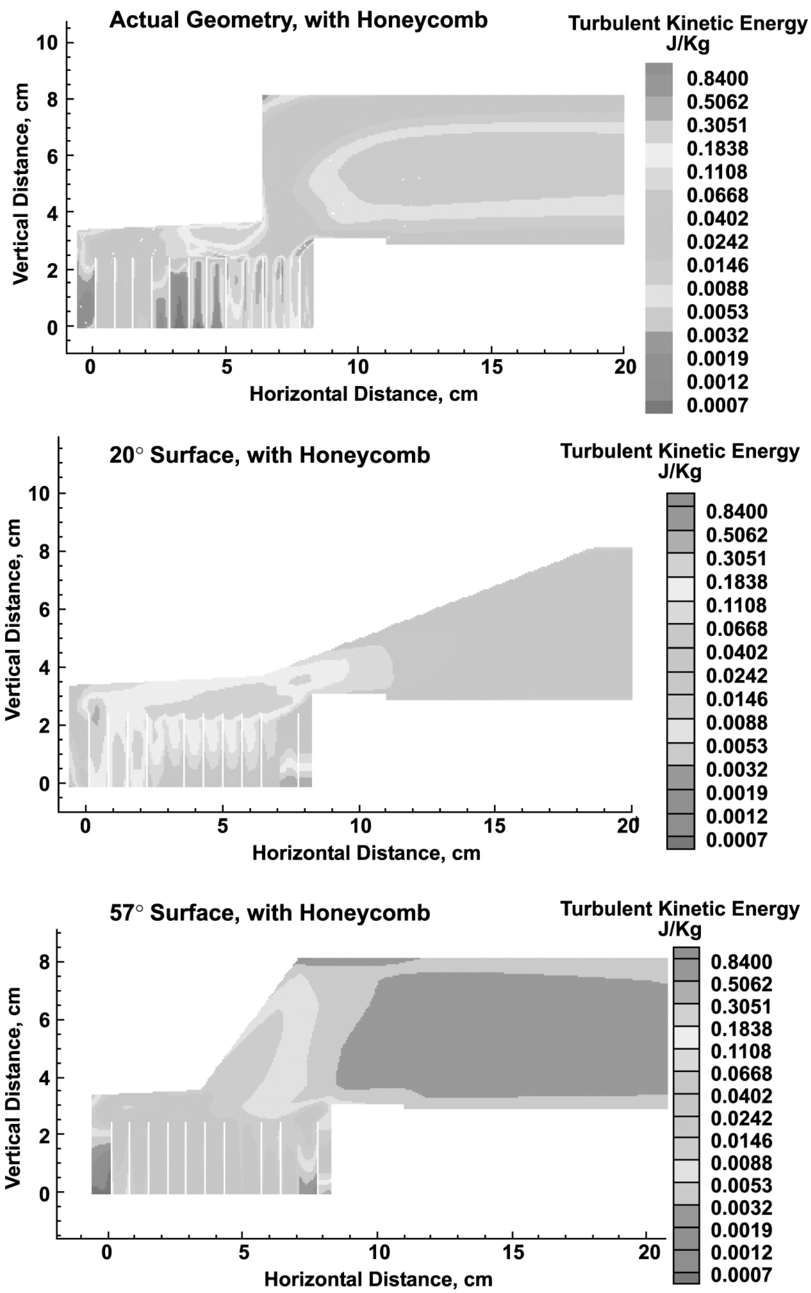

Figure 7.
Turbulent kinetic energy contours for a variety of geometries at the DAG region

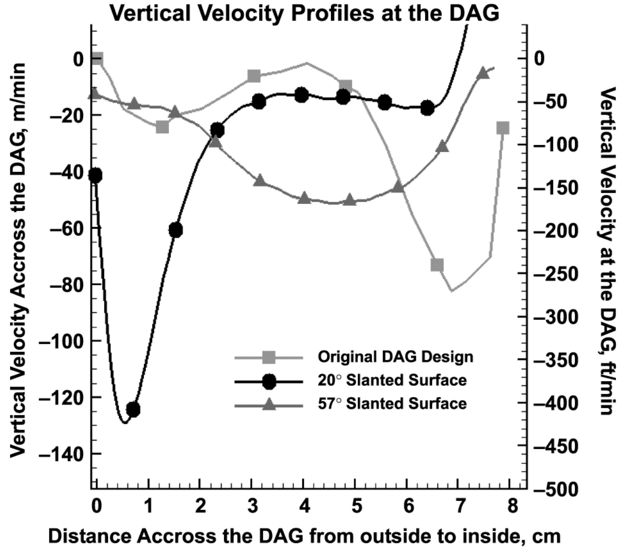

Figure 8.
Vertical velocity profile at the DAG for the all cases depicted in Figure 7

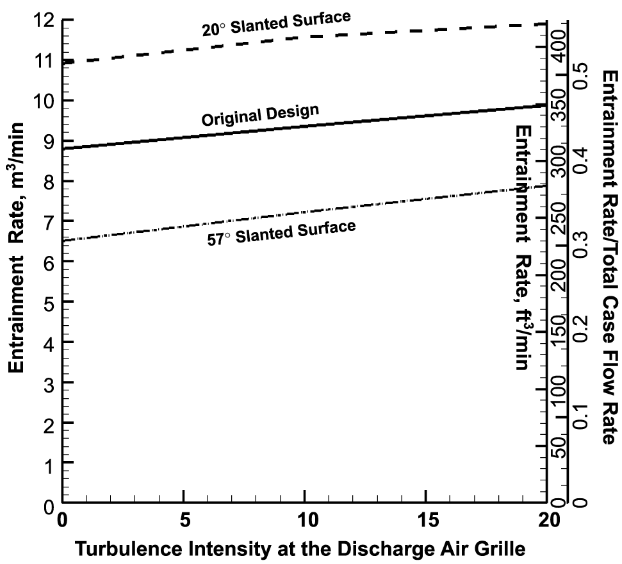

Figure 9.
Entrainment rate as a function of turbulence intensity at the DAG for different DAG design scenarios at the optimized $\mathrm{Re} = 3,400$

exit velocity at the DAG on the entrainment rate. We found that a skewed parabolic profile with the peak shifted towards the inner section of the case generates the minimum entrainment and demonstrates that with simple changes to the geometry of the DAG, we could achieve a significant reduction in the entrainment rate.

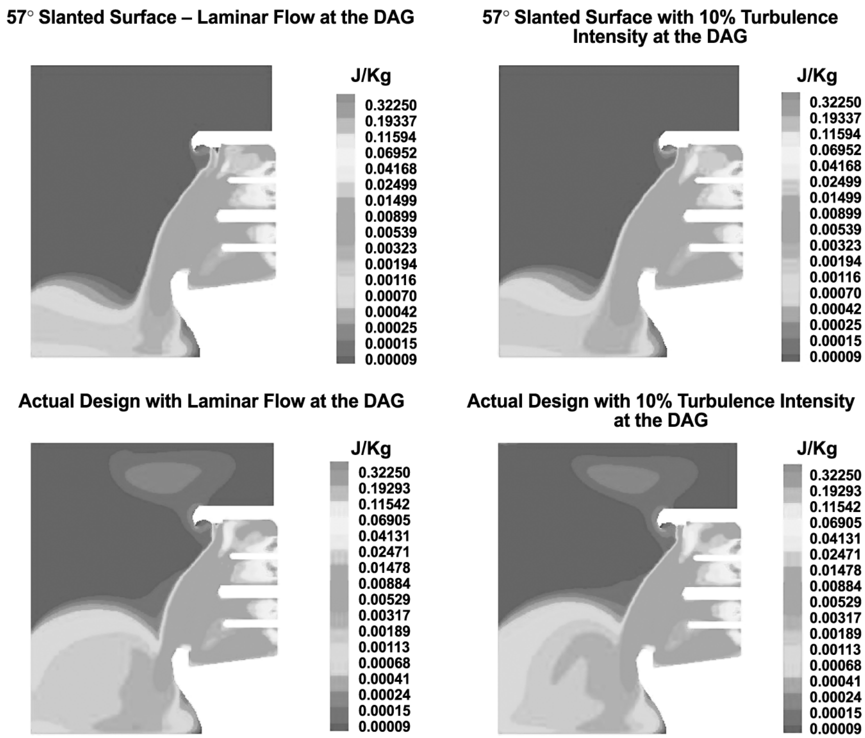

Figure 10.
Turbulence intensity contours for the proposed and actual cases with laminar and 10 percent turbulence intensity being imposed at the DAG

References

Field, B., Kalluri, R. and Loth, E. (2002), "PIV investigation of AIR-curtain entrainment in open display cases", paper presented at New Technologies in Commercial Refrigeration IIR Conference, Urbana, July.

Hetsroni, G., Hall, C.W. and Dhanak, M. (1963), "Heat transfer properties of an air curtain", *Trans. Of the ASAE*, pp. 328-34.

Howell, R.H. and Adams, P.A. (1991), "Effects of indoor space conditions on refrigerated display case performance", *ASHRAE – 596RP*, Department of Mechanical Engineering, University of South Florida, Tampa, FL, November 1991.

Navaz, H.K., Faramarzi, Ramin, Dabiri, D., Gharib, M. and Modarress, D. (2002), "The application of advanced methods in analyzing the performance of the air curtain in a refrigerated display case", *ASME J. of Fluid Engineering*, Vol. 124.

Navaz, H.K., Henderson, B.S., Faramarzi, R., Pourmovahed, A. and Taugwalder, F. (2004), "Jet entrainment rate in air curtain of open refrigerated display cases", *International Journal of Refrigeration*, Accepted for publication.

Stribling, D., Tassou, S.A. and Mariott, D. (1999), "A two-dimensional CFD model of a refrigerated display case", *ASHRAE Trans.*, pp. 88-94.

Further reading

Hetsroni, G. and Hall, C.W. (1963), *Further Studies of the Air Curtain*, Department of Agricultural Engineering, Westinghouse Atomic Power Div., Pittsburgh, PA, p. 438.

Corresponding author

Homayun K. Navaz can be contacted at: hnavaz@kettering.edu